

CHAPTER IV

INTERPRETATION AND CORRELATION

Petrographic Interpretation.

Results from regional observation indicate that the granitic rocks in Loei-Chiang Khan area are formed directly by magma differentiation. Magma differentiated by fractional crystallization processes, as suggested by the gradation of mafic minerals content. The gradation proceeds from the rock containing highly exclusive hornblende to biotite-hornblende, hornblende-biotite, solely biotite and finally to the rock containing rare mafic mineral. The QAP plot for the rocks containing hornblende to biotite hornblende (Figure 4-1) falls in syenitoid group. The rocks in this group are quartz monzonite (adamellite), quartz syenite and subordinate alkali-feldspar syenite. Whereas the rocks containing hornblende-biotite to biotite and even less mafic mineral fit in granitoid group (Figure 4-1). The rocks that contain hornblende and biotite content at the ratio about 1:1 (total mafic $Bi+Hbl \sim 15\%$) can be considered as transitional crystallization phase between syenitoids and granitoids (Figure 4-2). These rocks are hornblende biotite or biotite hornblende monzogranite and/or adamellite. The fine-grained granitic rocks with no or less mafic content fall in alkali-feldspar granite (Figure 4-3).

Petrographic results within the study area, Phu Sanao batholith, also represent similar sequences of crystallization. However, only exposed granitic rocks will

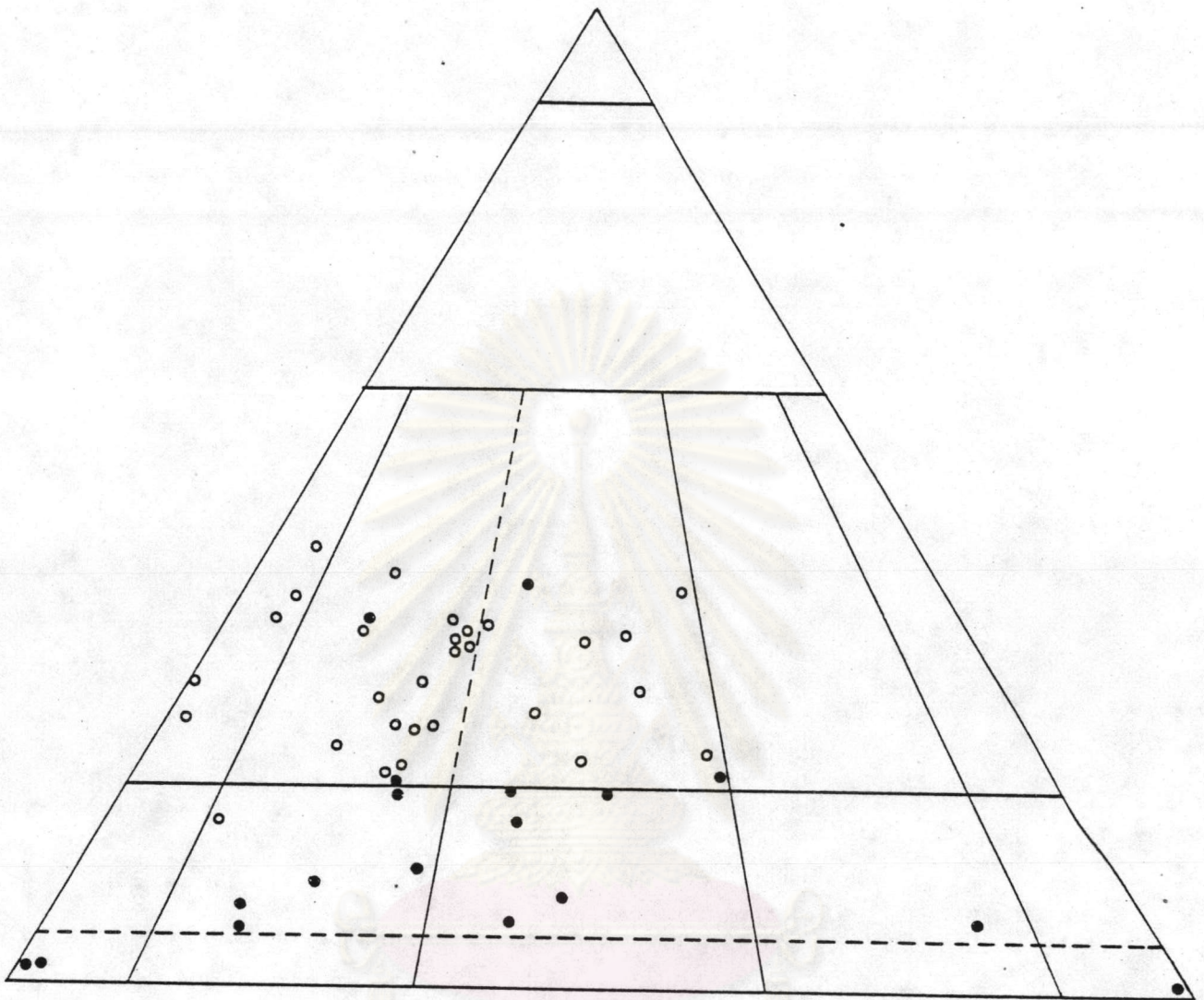


Figure 4-1. The QAP plot of the Loei-Chiang Khan granites, black circles illustrate syenitoid rocks containing mainly hornblende while white circles are granitoid rocks with mainly biotite to no mafic mineral contents.

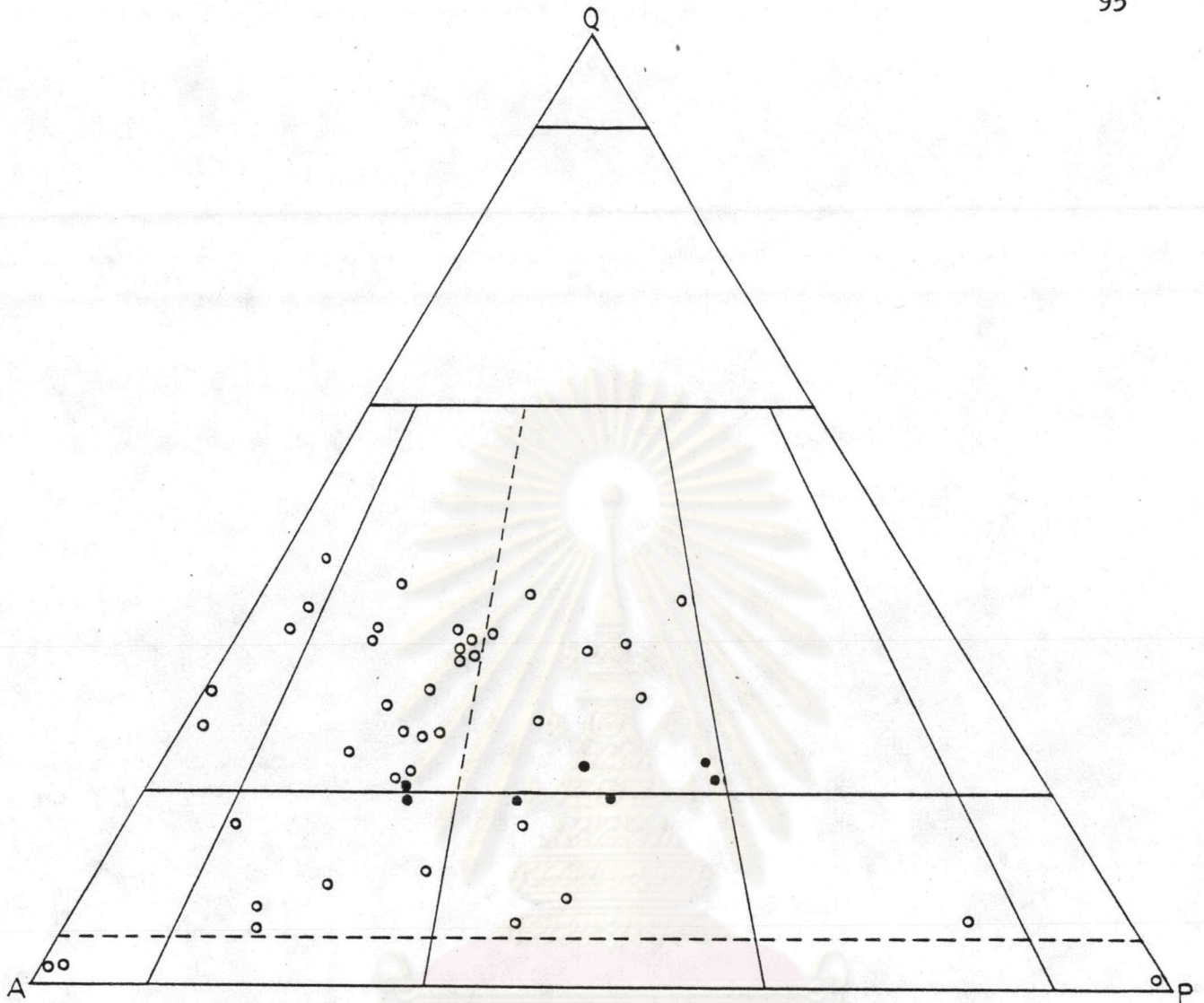


Figure 4-2. The QAP plot the syenitoid and granitoid rocks which composed of essential Hornblende-biotite or biotite-hornblende (black).

จุฬาลงกรณ์มหาวิทยาลัย

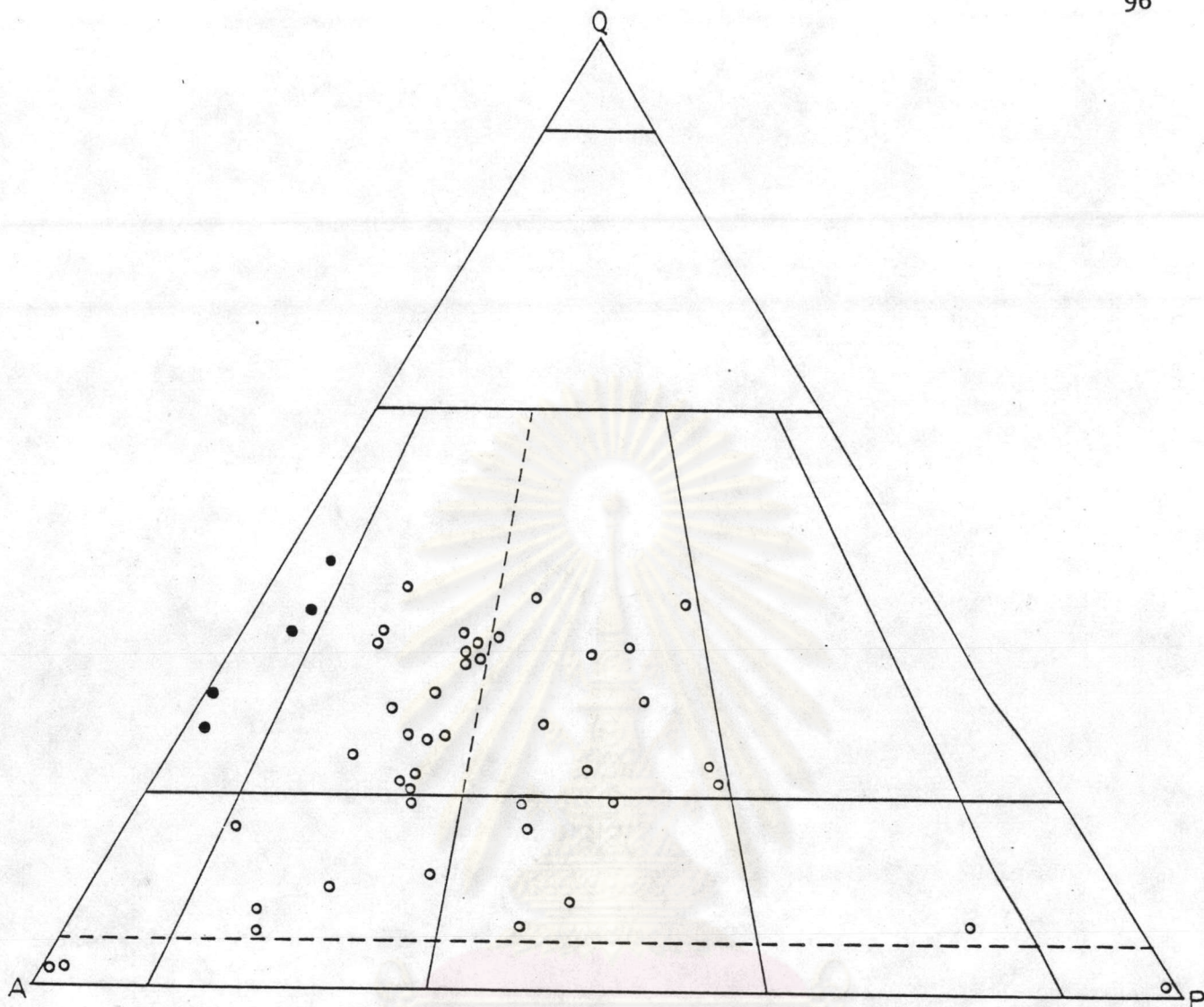


Figure 4-3. The QAP plot illustrates the alkali-feldspar granitic phase which composed less or no mafic mineral contents (black dot).

be concerned. Thus, the sequences within the area commence from hornblende-biotite monzogranite, granitoid phase in the Na Khaem subunit to biotite granite and/or less mafic content syenogranite in the Phu Sanao, Phu Lek subunits and finally to alkali-feldspar phase with no mafic content in Ban Kok Du subunit (Figure 4-4).

The tectonic environment of Phu Sanao batholith can be gained by using the tectonic environment diagram of Maniar and Piccoli (1989). The modal quartz-alkali feldspar and plagioclase plotting on this diagram reveals that the Phu Sanao granites are emplaced probably by post orogenic to continental epeirogenic uplift, rift relating and minor continental collision tectonics (Figure 4-5). The author believes that the Phu Sanao batholith intruded to emplace during late Upper Permian to early Lower Triassic (especially early Lower Triassic) according to the following evidences :

- 1) The cross-cutting relationship between Phu Sanao batholith and the main N-S trending Chiang Khan-Loei-Wang Saphung wrench fault (Lower to Middle Triassic).

- 2) The presence of Ban Na Muang-Ban Kok Du E-W reverse fault (Middle to early Upper Triassic) within the Phu Sanao batholith (Figures 2-7).

- 3) The western boundary of the batholith is parallel to the NE-SW strike slip fault (Lower Triassic). This may indicate intrusion is synchronous with the fault.

Microscopic-petrographic results also indicate dynamic tectonic of the Phu Sanao batholith (Plate 3-2,

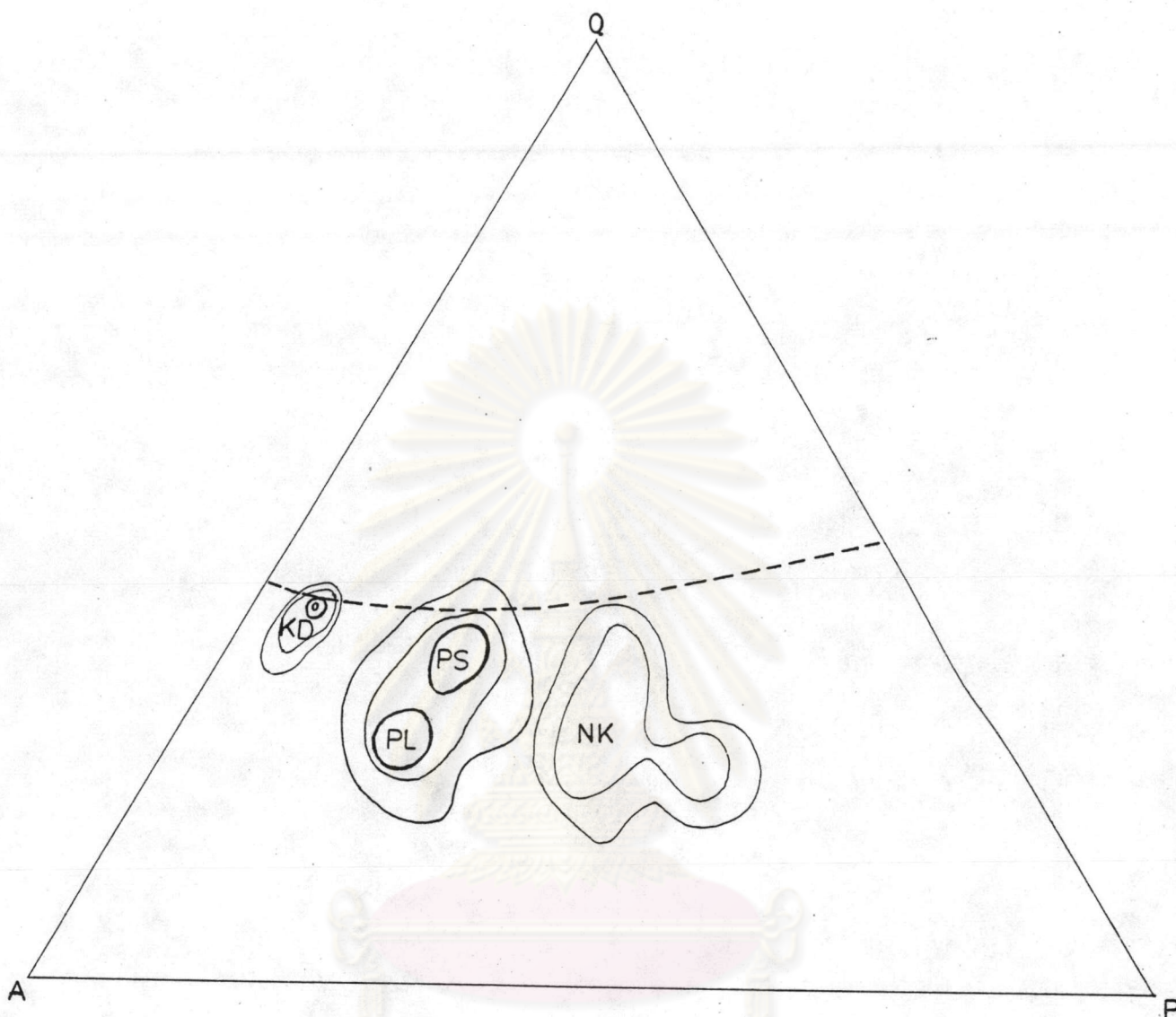


Figure 4-4. The QAP plot indicates the monzogranite (NK), syenogranite (PS and PL) and the alkali-feldspar granite (KD) crystallization phase.

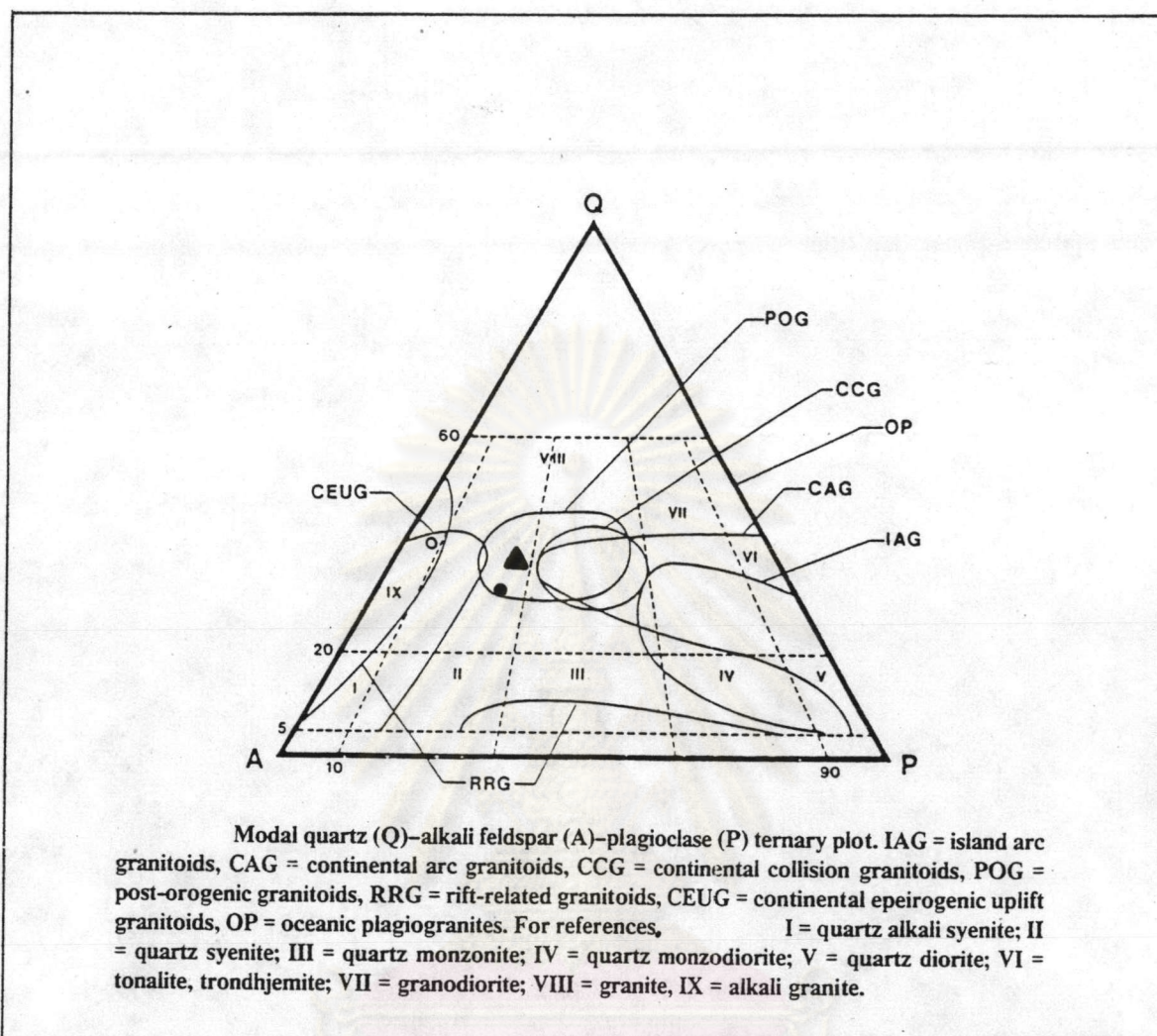


Figure 4-5. Plot of the Phu Sanao granites on Maniar and Piccoli tectonic environment diagram, co-tectitic PS-PL (Black circle), KD (white) and PS (triangle).

จุฬาลงกรณ์มหาวิทยาลัย

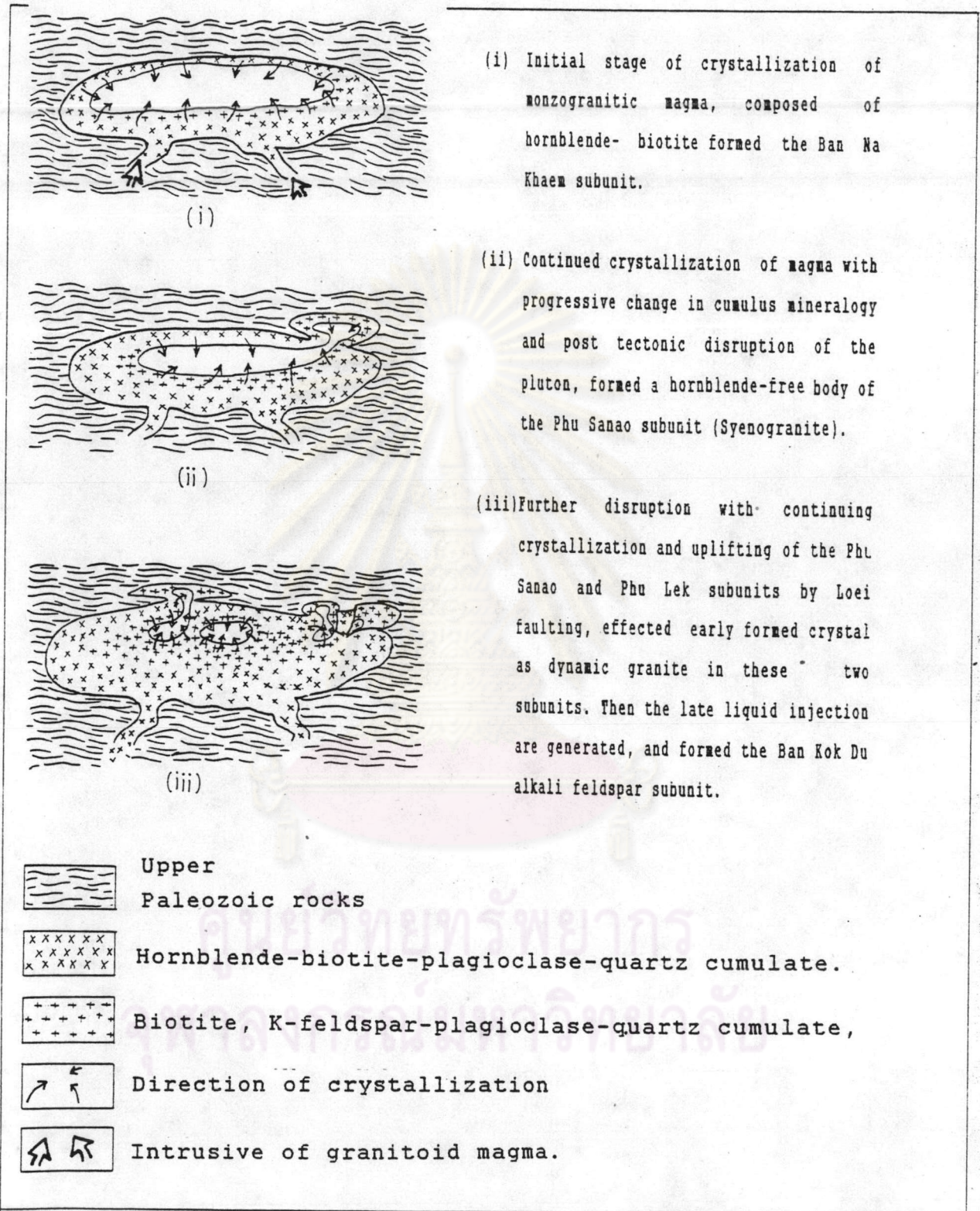


Figure 4-6. The generalize crystallization model of the Phu Sanao batholith.

Plate 3-3). They show dynamic or stress features within the granites of the Phu Sanao and the Phu Lek subunits.

In addition to tectonic environment and structural evidences, the author would like to point out that at least there are three disruptions of magmatic crystallization are involved. The first one is the emplacement of post-orogenic Phu Sanao batholith simultaneously with NE-SW conjugate strike-slip faults. The second is post-tectonic uplift (continental epirogenic uplift) of the Phu Sanao subunit (Lower to Middle Triassic) by the main N-S Loei wrench fault. And the third is the progressive disruption uplift of Ban Kok Du subunit generated by the E-W Kok Du-Na Muang reverse fault. The generalized crystallization model of the Phu Sanao batholith is presented in Figure 4-6.

Engineering Correlations

The petrographic and engineering properties of the Phu Sanao granite could be related through graphic plots. Some certain parameters may be established by curve fitting either method of linear regression or exponential one. Hence, one property parameter could lead to another one. The unconfined compressive strength (UCS) is one of the most important rock properties in engineering aspect. However, the difficulty in preparing a core sample causes limiting number of testing. Fortunately, the UCS of the Phu Sanao granite shows distinctive linear relationship to point load strength index (Is 50) (Figure 4-7). The Is 50 determination is easier to perform on irregular specimens. The UCS can be expressed as linear equation.

$$\text{UCS} = 5.8 + 19.4 \text{ Is } 50 \quad (4-1)$$

This equation is very close to the Broch and Franklin's (1972) approximation. They estimated UCS as 24 Is 50. Figure 4-8 provides the exponential curve fitting between LA percentage of wear and the UCS. Therefore, if the UCS of granites is known, the percentage of wear of the rocks used as construction aggregate can be predicted through this following equation.

$$\text{LA percentage of wear} = (4.4)(0.0047)^{\text{UCS}} \quad (4-2)$$

Nevertheless, the uniformity (UF) listed in table 3-5 indicates that aggregates from these granitic rocks are less uniform hardness.

The weathering decomposition parameter (xd) also shows significant relationship to the UCS. Figure 4-9(d) illustrates the Xd-UCS curve fitting of entire Phu Sanao granites while Figure 4-9(a-c) show the separated relation of Phu Sanao, Phu Lek and Ban Kok Du subunits respectively. These curves establish similar fitting despite the lithologic difference. The UCS of Phu Sanao granite can be estimated from Xd parameter as :

$$\text{UCS} = (5.1)(-2.49)^{\text{xd}} \quad (4-3)$$

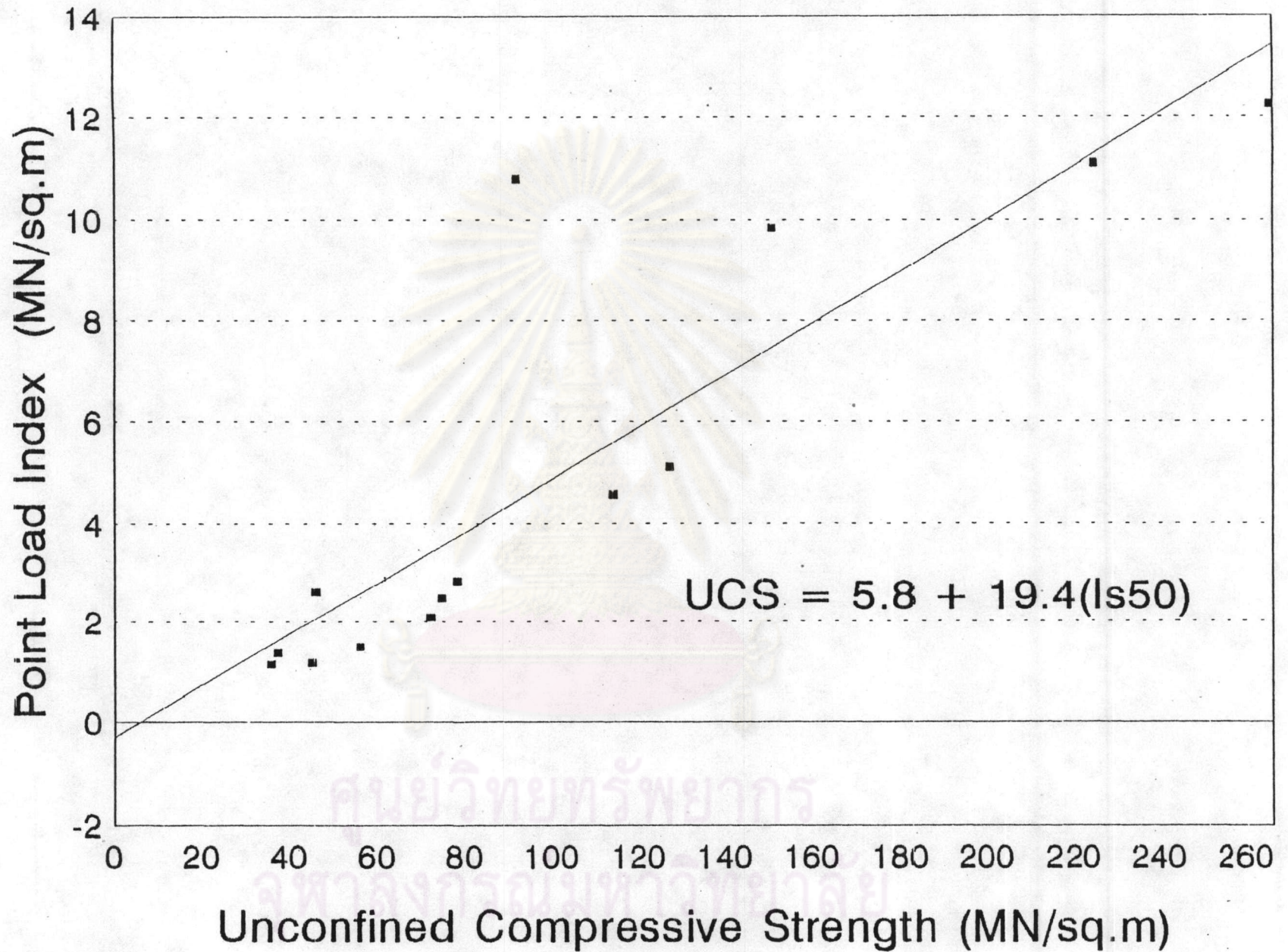


Figure 4-7. The plot of unconfined compressive strength versus point load strength index shows linear relationship.

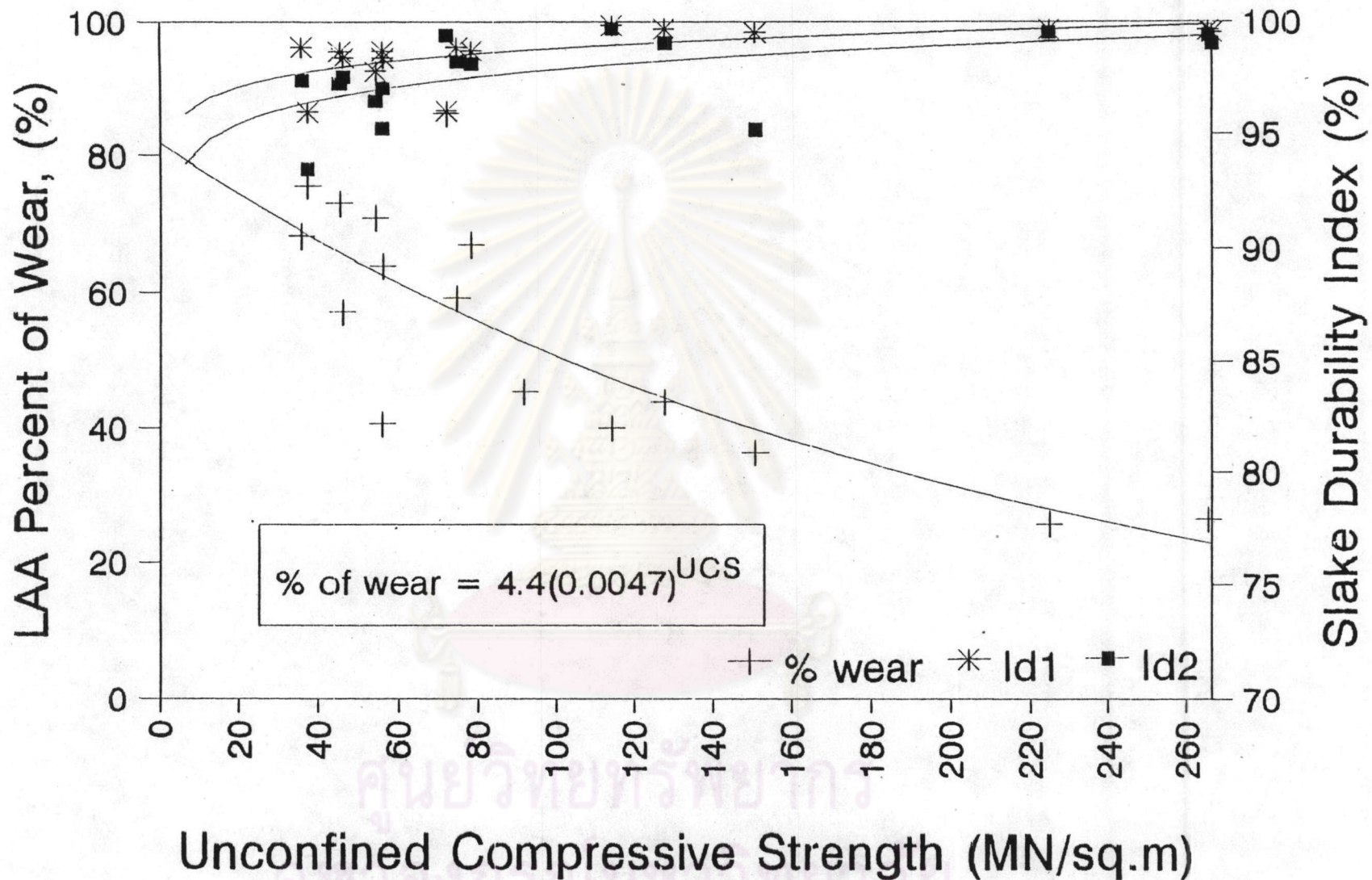


Figure 4-8. The comparison curves of unconfined compressive strength to abrasiveness and slake durability of Phu Sanao granites.

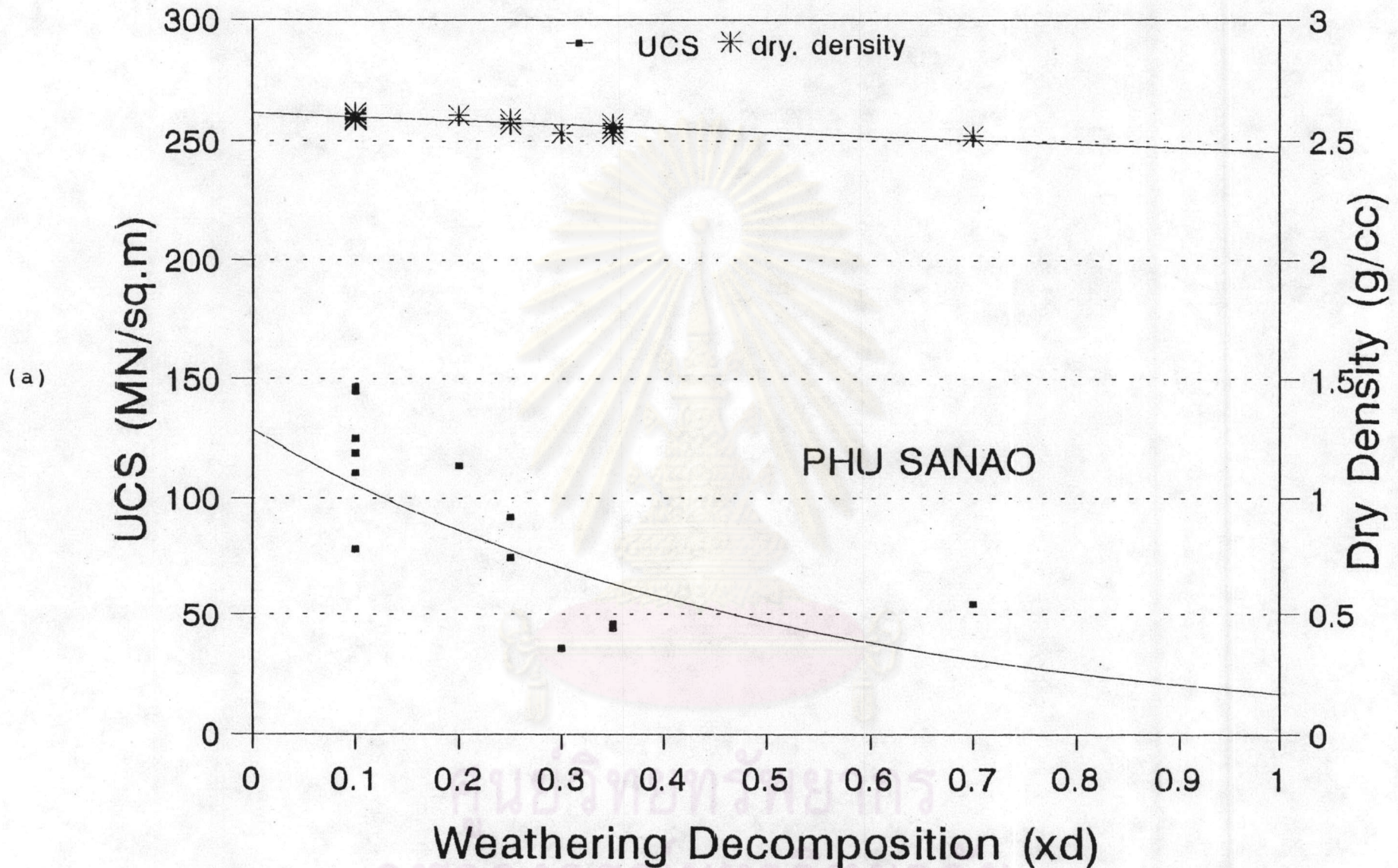


Figure 4-9. The plot of strength, bulk density relates to weathering decomposition of the Phu Sanao granites. (a) The Phu Sanao subunit, (b) Phu Sanao and Phu Lek subunits, (c) Ban Kok Du subunit, (d) integrated of the Phu Sanao, Phu Lek and Ban Kok Du subunits.

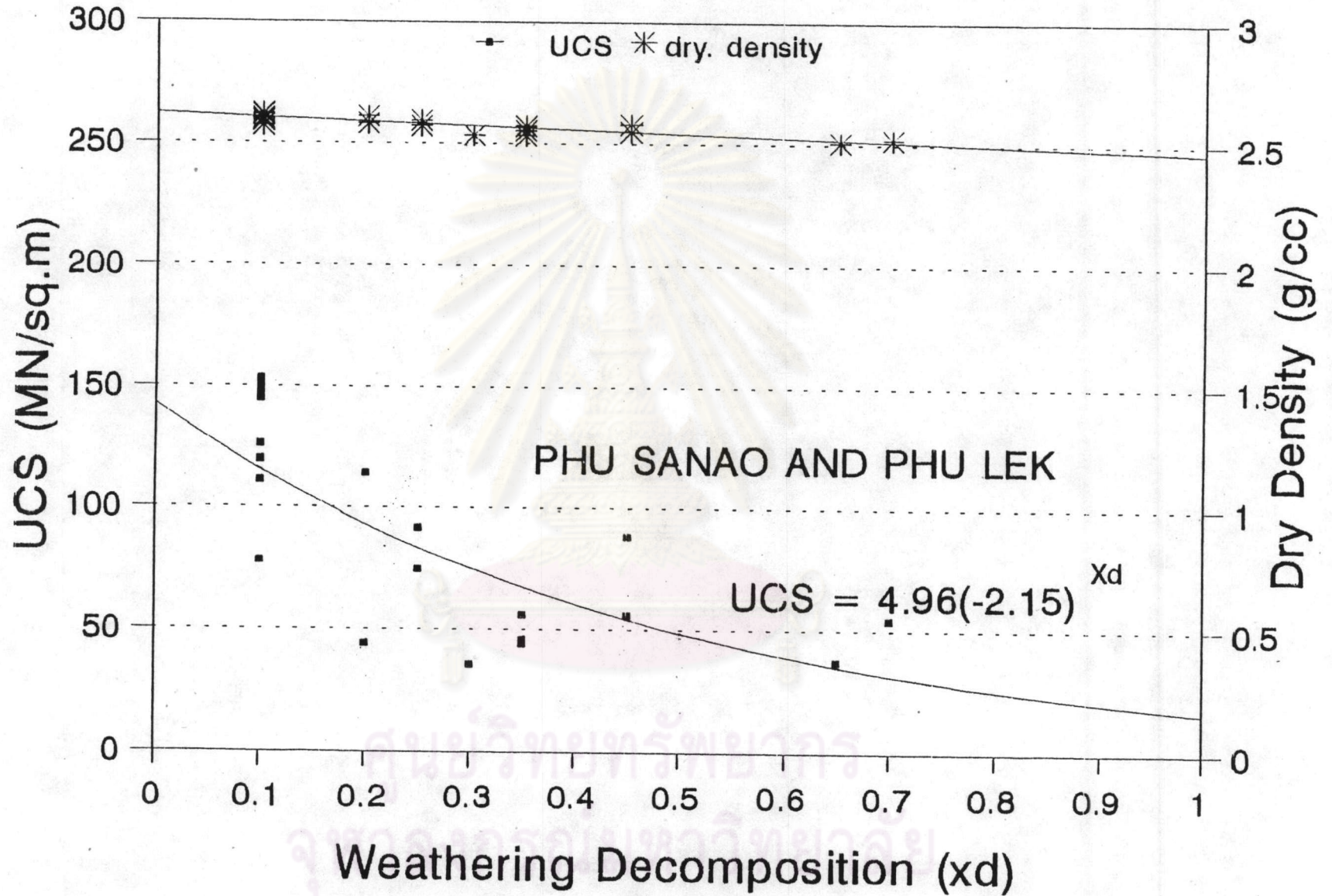


Figure 4-9. (Cont.)

(b)

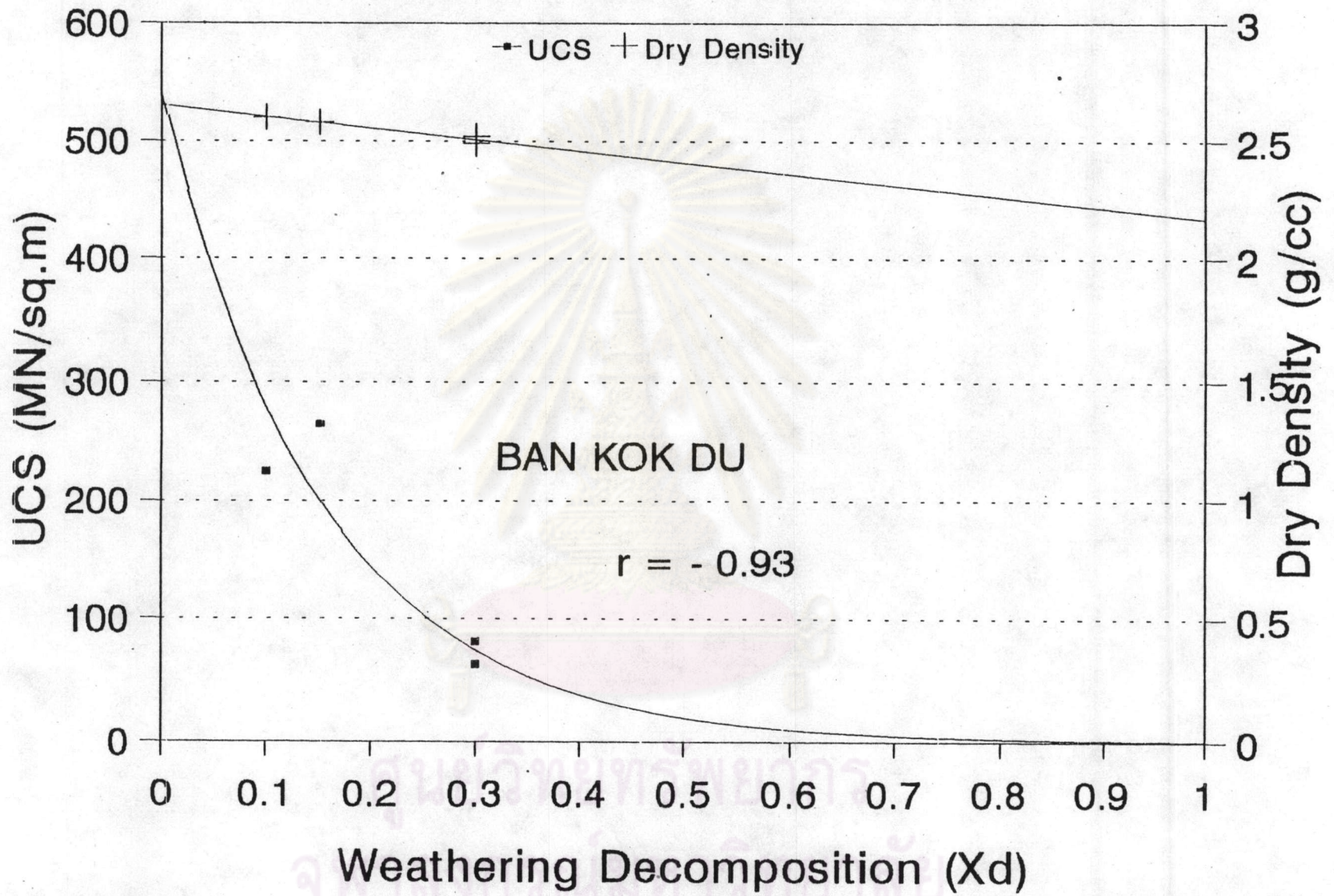


Figure 4-9. (Cont.)

(c)

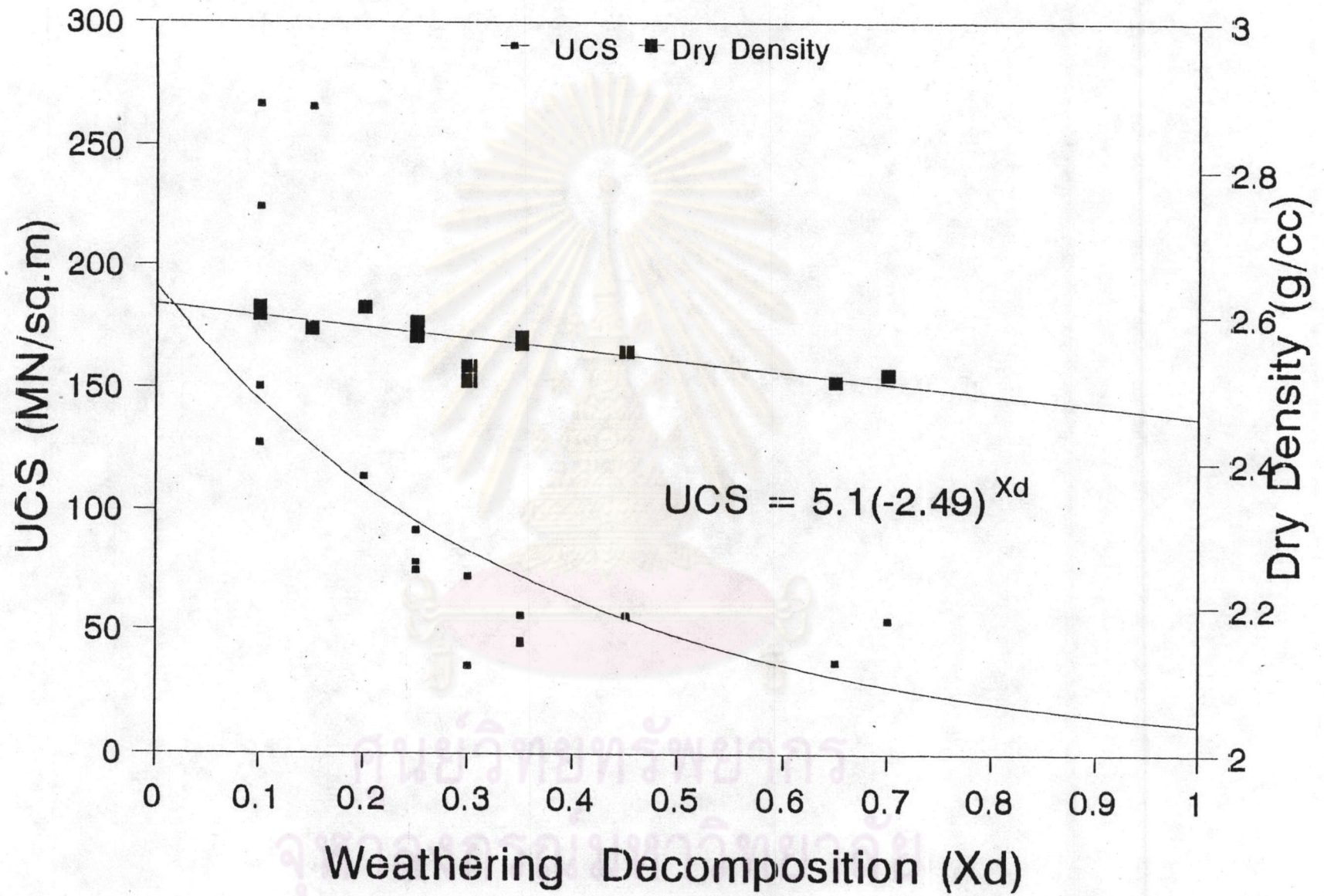


Figure 4-9. (Cont.)

(d)

The porosity (n) of these rocks can be used as a parameter to evaluate strength and abrasiveness (Figure 4-10 and Figure 4-11) as well.

$$\text{UCS} = 5.19 (-0.23)^n \quad (4-4)$$

$$\text{LA percentage of wear} = 3.49 (0.13)^n \quad (4-5)$$

In addition, the porosity also has some relation to X_d value as

$$X_d = (-2.02)(0.21)^n \quad (4-6)$$

Mineral composition contents have insignificant effect on the strength of the rocks (Figure 4-12). Nevertheless, the increasing K-feldspar and decreasing in plagioclase contents lead to higher rock strength. Fine-grained granitic rocks give higher strength value than coarse-grained ones. (Figure 4-13, 4-14). Though the grain contact characteristic shows inadequate effect to the strength, the rocks with higher concave-convex contact with lower straight contact tend to have higher strength (Figure 4-15).

The slake durability (Id_1 and Id_2) of these granitic rocks depend mostly on the weathering

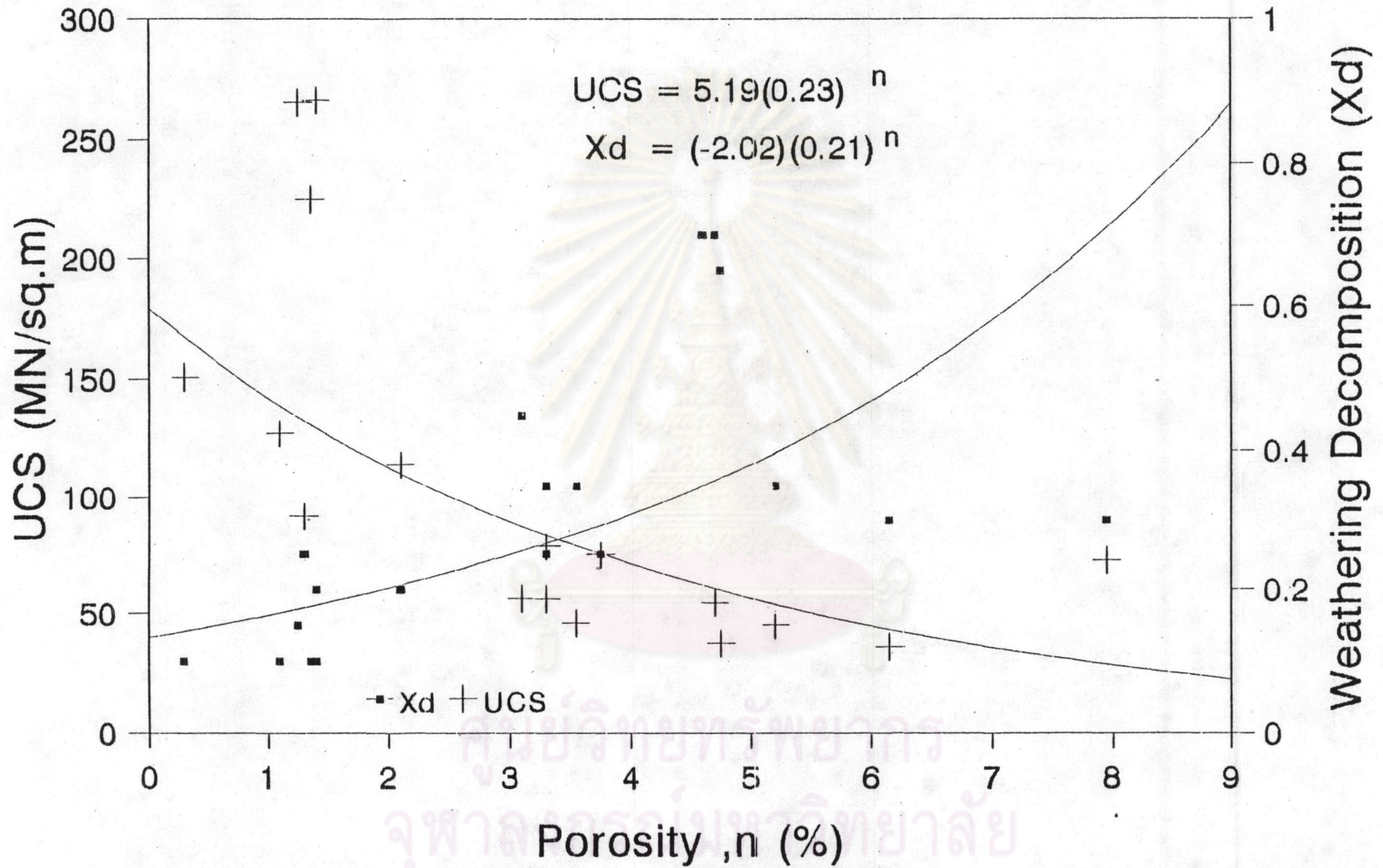


Figure 4-10. The curves of porosity to unconfined compressive strength, and to weathering decomposition of Phu Sanao granites.

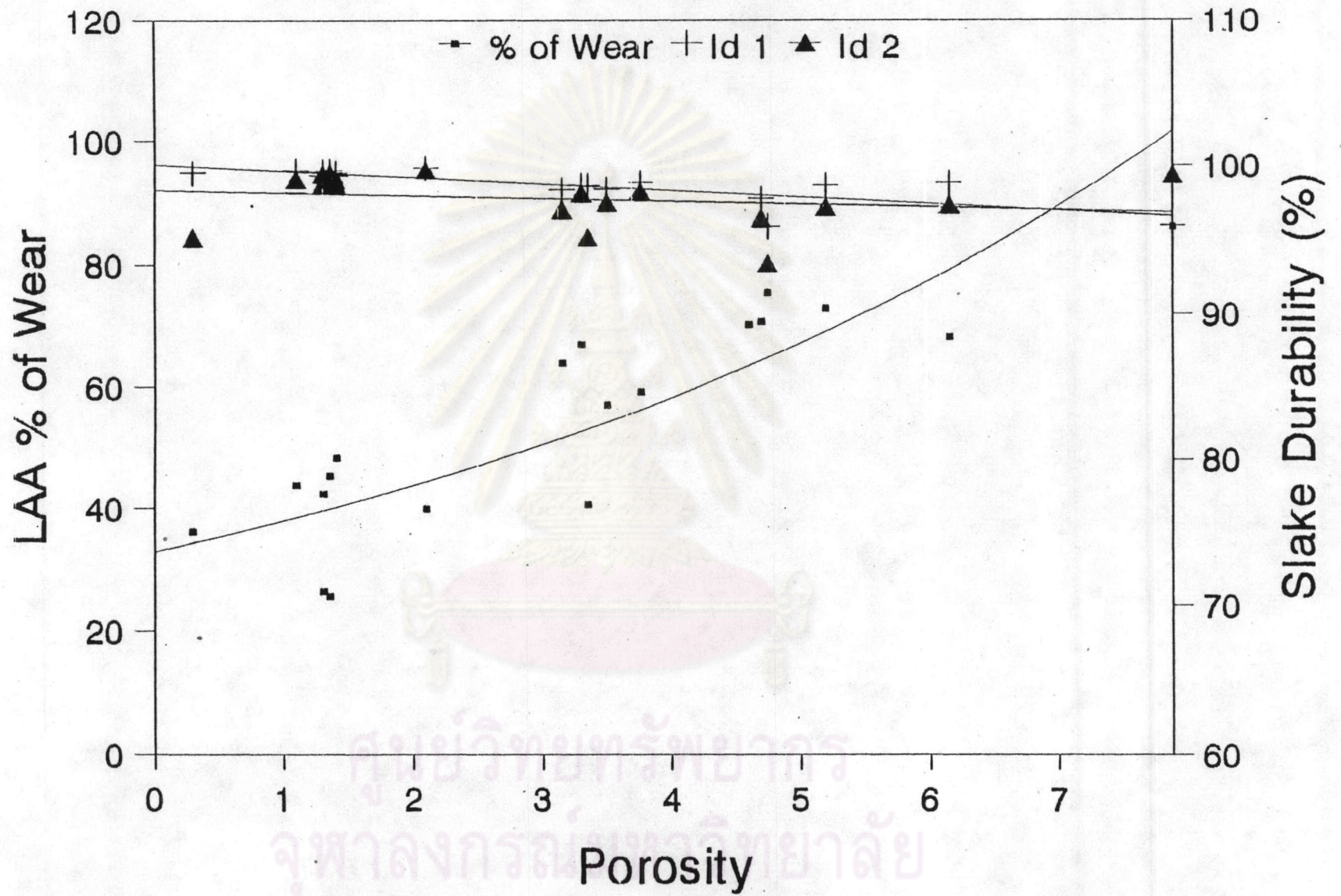


Figure 4-11. The porosity correlates to percentage of wear and slake durability of Phu Sanao granitic aggregates.

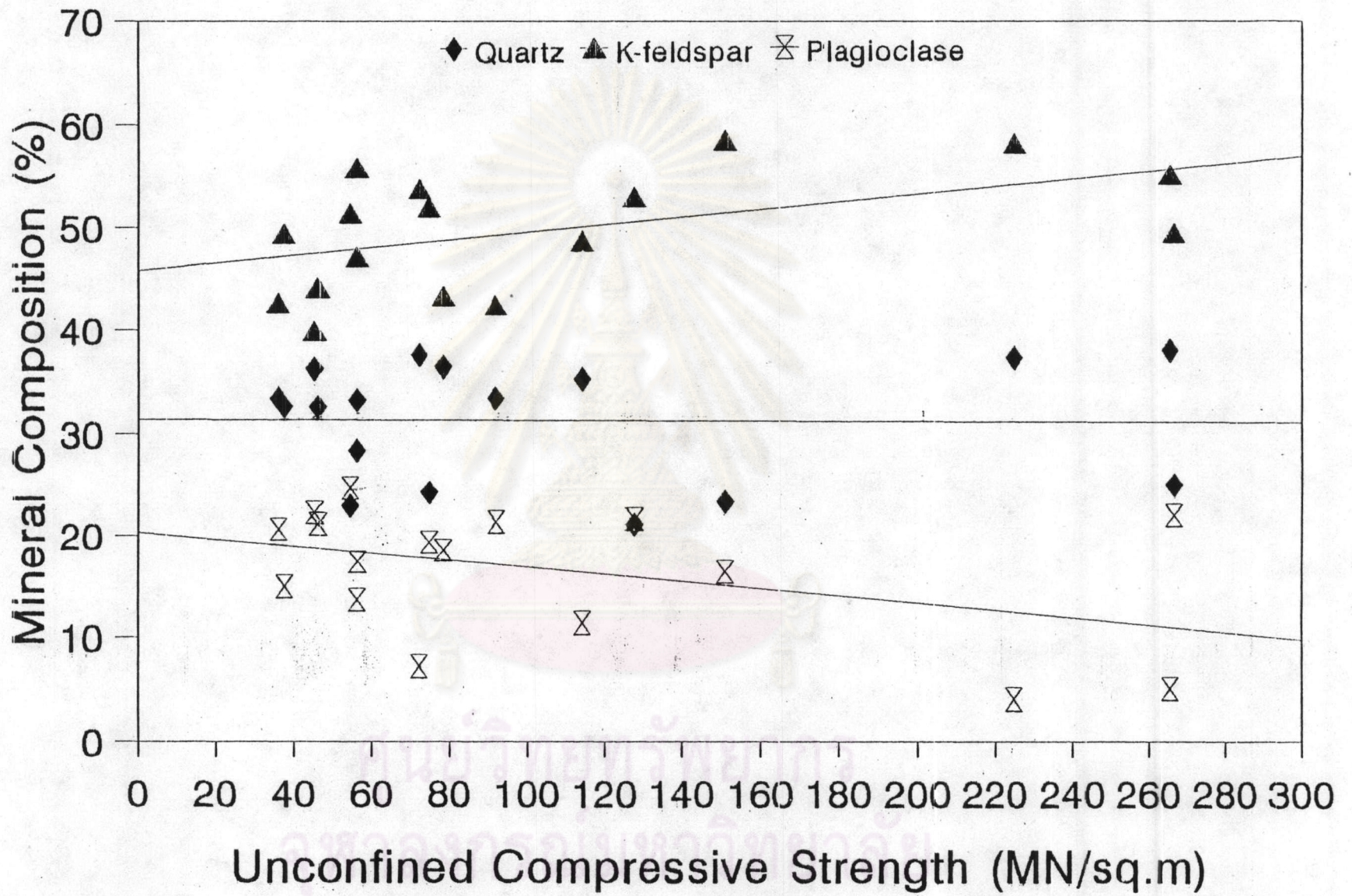


Figure 4-12. The plot of quartz, K-feldspar and plagioclase contents correlates to unconfined compressive strength.

decomposition, porosity, and strength of the rocks (Figure 4-8, 4-11). The above correlations draw to the conclusion that unconfined compressive strength of the Phu Sanao granites varies from 35 to 266 MN/sq.m. These range of strength values could be classified into weathering grade description as in Figure 4-16. The correlation coefficient of each property is tabulated in Table 4-1.



ศูนย์วิทยทรัพยากร
จุฬาลงกรณ์มหาวิทยาลัย

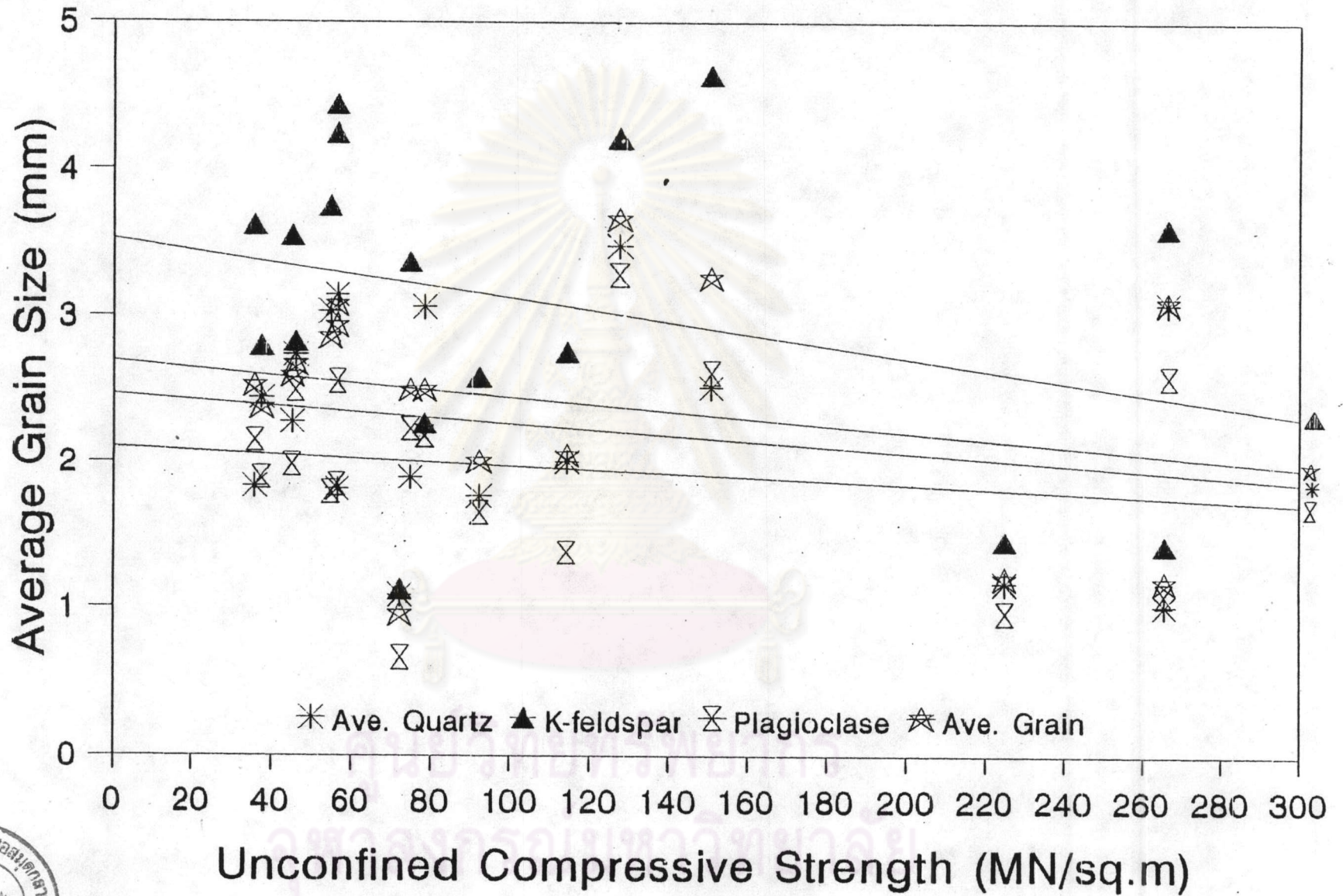


Figure 4-13. The plot showing unconfined compressive strength trending based upon average grain of quartz, K- feldspar, plagioclase and total average grain sizes.



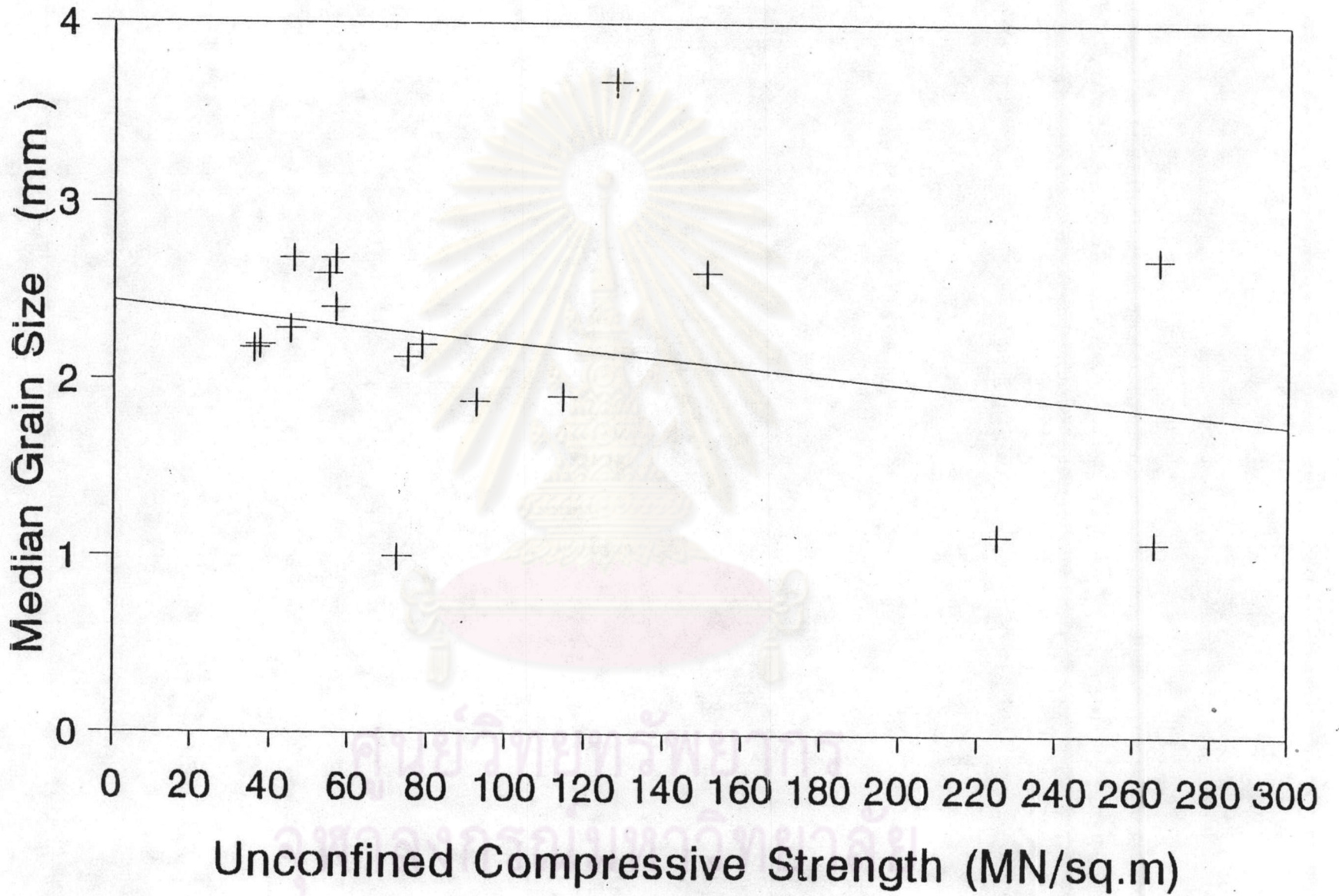


Figure 4-14. The plot of unconfined compressive strength related to median grain of Phu Sanao granites.

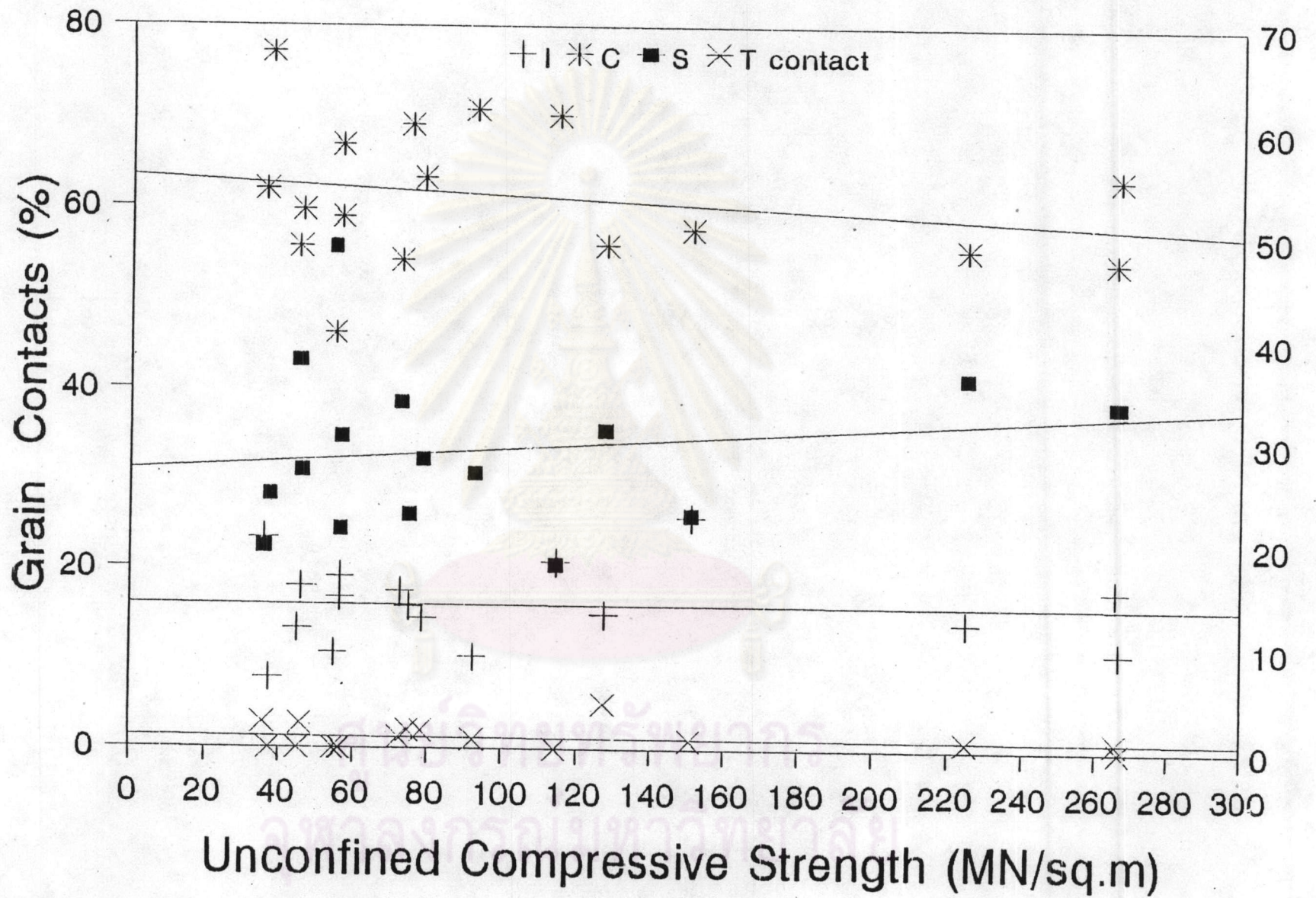


Figure 4-15. The plot between grain contacts and unconfined compressive strength of Phu Sanao granites.

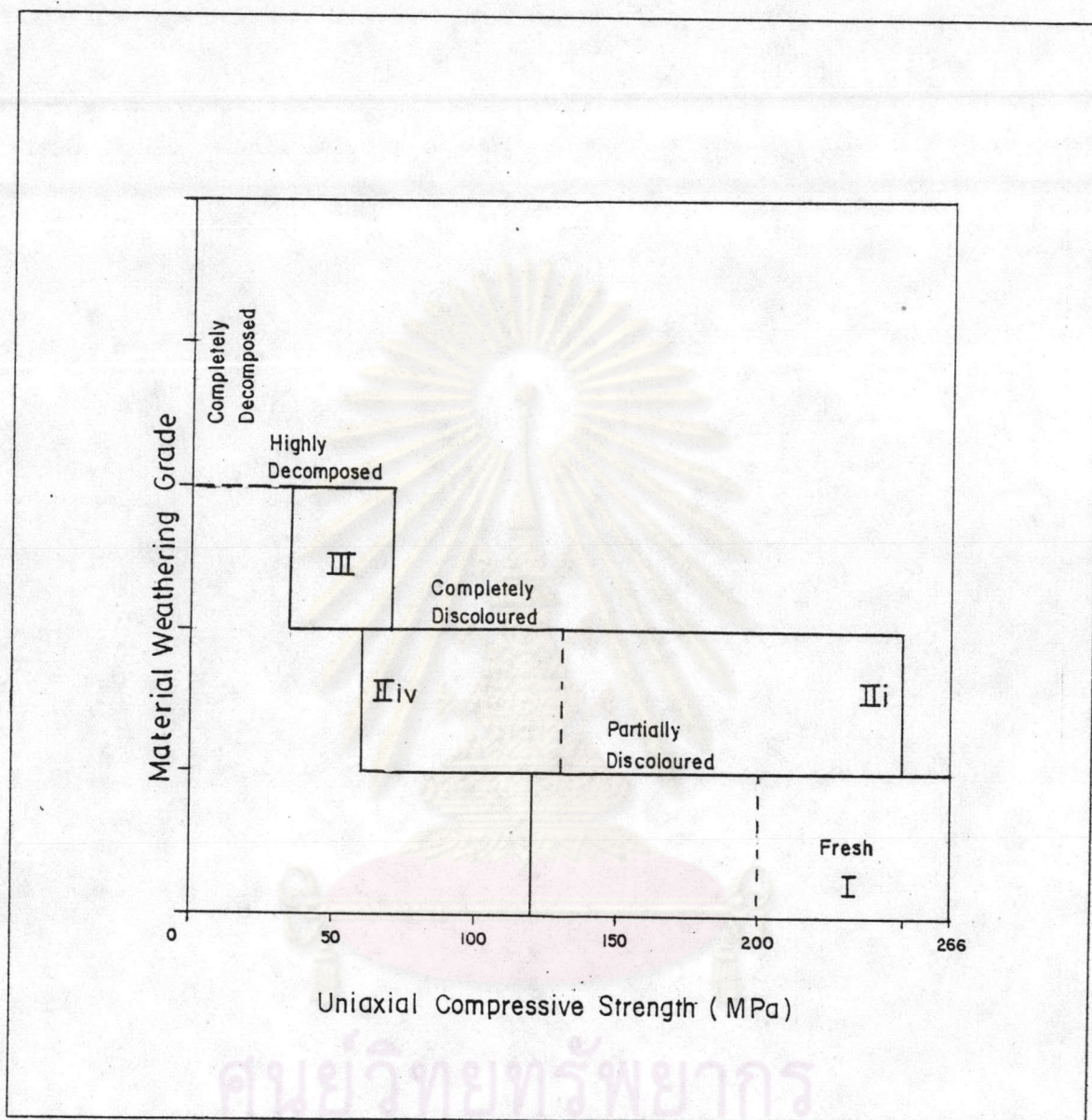


Figure 4-16. The unconfined compressive strength ranges with various weathering grades.

Table 4-1. The correlation coefficient of Phu Sanao Granites

Index Parameter	Compared to	Correlation coefficient (r)
IS 50	UCS	0.867
LA % of wear		-0.794
Id ₁		0.571
Id ₂		0.517
Q Quartz contents		-0.01
k k-feldspar contents		0.497
P Plagioclase contents		-0.433
X Average grain size		-0.253
Q Quartz grain size		-0.210
k k-feldspar grain size		-0.292
P Plagioclase grain size		-0.153
I-contact		-0.010
C-contact		-0.200
S-contact		0.20
T-contact		-0.065
UCS (entire samples)	Xd	-0.678
UCS of PS		-0.716
UCS of PS & PL		-0.740
UCS of PL		-0.818
UCS of Kd		-0.931
Xd	porosity	0.590
UCS		-0.661
LAA		0.877
Id ₁		-0.779
Id ₂		-0.213

ศูนย์วิทยทรัพยากร
จุฬาลงกรณ์มหาวิทยาลัย